JOURNAL OF APPLIED ELECTROCHEMISTRY 19 (1989) 777–783

Anodic behaviour of copper electrodes containing arsenic or antimony as impurities

JULIO C. MINOTAS, HOCINE DJELLAB, EDWARD GHALI

Université Laval, Département de mines et métallurgie, Québec, G1K 7P4, Canada

Received 9 June 1988; revised 10 January 1989

The anodic behaviour of three different copper electrodes in sulphuric acid medium was investigated using cyclic voltammetry in the potential range between the rest potential $E_{i=0} = -0.34\,V$ and $+0.80\,V$ vs the Hg, Hg_2SO_4/K_2SO_4 saturated (MSE) reference electrode. Arsenic dissolved in the electrode matrix as well as oxygen dissolved in solution were found to delay passivation. The anodic peak current density was proportional to the square root of the potential sweep rate in two consecutive domains. An unusual break was observed for high scan rates ($> 50\,mV\,s^{-1}$) and was attributed to an increase of the medium viscosity because of the large gradient of concentration near the electrode surface. On the other hand, current oscillations, usually observed in the anodic processes of metallic electrodes, have been studied as a function of the electrode vertical/horizontal positions. Gravity has been found to affect both the frequency and the amplitude of the oscillations. X-ray diffraction measurements conducted on galvanostatically electrolyzed samples revealed, besides copper metal, the presence of copper sulfate pentahydrate and trihydrate for Cu–As and Cu–Sb, respectively. SEM analysis showed the existence of preferential domains of white product on a darker background of metallic copper or copper oxides.

1. Introduction

Copper electrorefining was one of the first electrometallurgical processes used in industry. Even though it was established in the late years of the nineteenth century (1871) [1], a number of operational and fundamental problems remain unsolved. The mechanism of the anodic oxidation of copper in copper sulphate–sulphuric acid electrolyte is as yet insufficiently understood. One area of practical concern is the passivation of copper anodes. In spite of the electrochemical nature of the problem, little information has been published on the anodic passivation of copper in industrial electrorefining conditions. Anodic passivation has been one of the major problems encountered by copper refineries [2–4].

Many hypotheses concerning the mechanism of copper passivation in different media have been given in the literature [3–6]. The most generally acknowledged mechanism is the precipitation of copper sulphate following a dehydration of the layer adjacent to the electrode surface [3, 6]. In this regard, scant attention has been paid to the role of water as related to the copper dissolution process, although it seems evident that significant amounts of water are required for solvation. On the other hand, copper sulphate has been detected on non-passivated electrodes [7, 8]. It appears then, that although the formation of a partially soluble non-conductive surface layer of copper sulphate might be a necessary step, it is not sufficient by itself to explain the passivation mechanism.

Some insoluble compounds such as silicates, copper silver selenides, or copper and nickel oxides have already been reported for industrial anodes [9, 10]. The accumulation of those insoluble entities on the active area of the electrode leads to the formation of a thick passivating slime layer [11, 12]. For instance, the presence of high concentrations of nickel in the electrode matrix results in the precipitation of nickel oxide particles on copper which accumulate in the slime layer [13].

The present paper describes a cyclic voltammetric investigation of the anodic behaviour of copper electrodes containing traces of either arsenic or antimony. We first focused our efforts on arsenic and antimony which are commonly encountered in industrial anodes and are reportedly of great importance in the electrorefining process [9, 12]. The desired metal was introduced in electrolytic pure copper at concentrations in the impurity level. The contribution of each of these two elements (arsenic and antimony) to anodic passivation was evaluated separately. The oscillatory phenomena, which have been observed using a number of electrochemical methods, have also been considered in the present investigation. X-ray diffraction measurements and SEM analysis were used in order to examine the anodically polarized surfaces.

2. Experimental details

2.1. *Reagents and electrolyte preparation*

All the chemicals used during this investigation were ACS reagent grade and used without further purification. Doubly distilled deionized water ($\sigma = 5 \times 10^{-6}\,\Omega^{-1}\,cm^{-1}$) was used as the solvent. The com-

0021-891X/89 $03.00 + .12

position of the electrolyte solution, chosen according to typical industrial conditions, was as follows: 1.66 M (167 $g l^{-1}$) sulphuric acid, 0.29 M (17 $g l^{-1}$ Ni^{2+}) nickel sulphate hexahydrate and 0.66 M (42 $g l^{-1}$ Cu^{2+}) copper sulphate pentahydrate.

2.2. *Electrode preparation*

Cu–Sb and Cu–As alloys were prepared using the following procedure: 99.8% pure electrolytic copper (OFHC grade) (Aldrich), cut into small pieces, was placed in a graphite crucible which was subsequently placed in a vacuum stock induction furnace. The atmospheric oxygen was removed by vacuum pumping and purging the furnace with dry argon. The crucible was heated by applying an HF induction current to reach the copper melting point. Gold label antimony or arsenic (Aldrich) wrapped in a pure copper foil was added to the molten copper, using a remotely controlled arm. The mixture was maintained at ca 1150° C for 3–5 min in order to allow impurities to diffuse and homogenize within the copper matrix. The molten metal was poured into a graphite mold giving 1.27 cm diameter cylindrical shaped bars, which were subsequently reduced to smaller diameter rods (1.25 cm). The graphite-made mold and crucible were used in order to reduce the amount of O_2 in the samples. Graphite reduces oxygen to form carbon dioxide gases. The sample compositions, estimated by atomic absorption spectroscopy, were respectively 0.15% and 0.055% (w/w) in As and Sb and were well distributed within the copper matrix, as can be seen from the photomicrographs of Fig. 1. No more than 11 ppm of oxygen were detected.

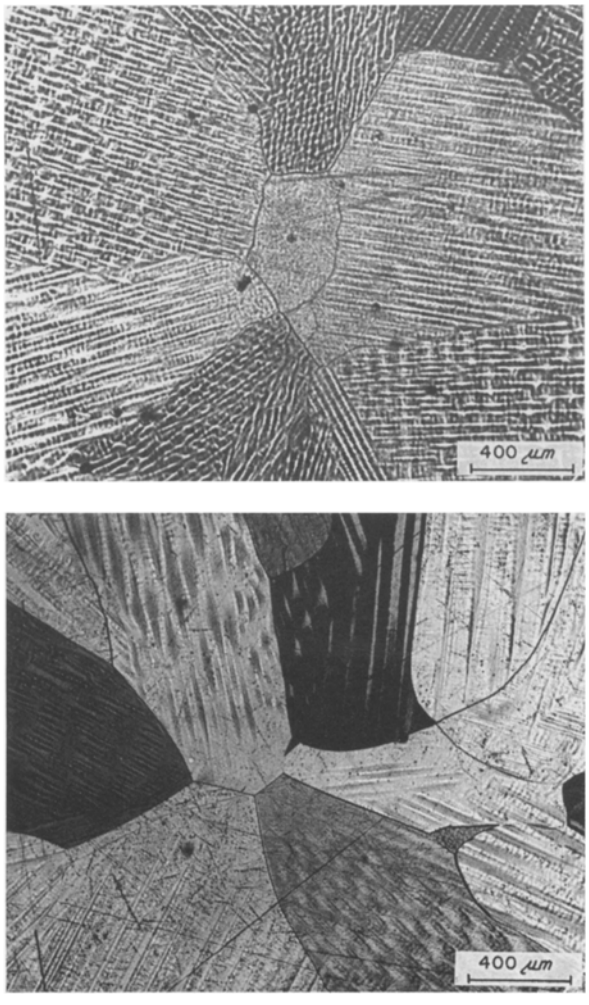

Fig. 1. Optical photomicrographs of Cu–0.15% As and Cu–0.055% Sb samples.

Small samples (1 cm length) were mounted in a protective coating consisting of an insulator, acrylic resin (Buehler), leaving only a circular working electrode area. The electrical contacts were made via copper wire leads connected to the working electrode using a 1 : 1 Pb–Sn welding alloy.

Prior to any experiment, the electrodes were polished using emery paper of various grades (from 100 to 600 μm grit), followed by cleaning and extensive rinsing with distilled water and ethanol in order to remove the oily polishing product. Since experimental results were not affected by the final polishing grade, mirror finishing was not used.

A larger area of electrolytic copper (2.84 cm^2), mounted in the same manner as the working electrode, was used as a counter electrode.

All potentials were referred to the Hg, Hg_2SO_4/K_2SO_4 saturated (MSE) reference electrode (0.64 V vs NHE) (Ingold Inc.) connected to the main cell by a thin bridge filled with the supporting electrolyte and terminating in a Luggin capillary. In order to minimize the ohmic drops, the tip of the capillary was always positioned at about 1 mm from the working electrode. Despite this effort, noticeable *IR* drops were always observed on the cyclic voltammograms.

2.3. *Cell and electrode mounting*

A high capacity (1 dm^3) double-walled glass container was used as an electrochemical cell. The counter and working electrodes were mounted at a fixed distance (ca 2 cm) from one another using a Teflon holder. Unless otherwise indicated, the working and counter electrodes were set in vertical positions.

The temperature of the solution was controlled and maintained by circulation of water at the desired temperature through the cell. This was controlled using a T-523 type Heto Brikerod thermostat, and maintained at 65.0 $\pm$ 0.5° C.

2.4. *Instrumentation*

All the electrochemical tests were carried out using a model RDE-4 bipotentiostat (Pine Instruments Co.) coupled with a model 530 *XY* recorder (Honeywell) in parallel to a 3476A digital multivoltmeter (Hewlett-Packard).

For X-ray diffraction analysis (XRDA), the specimens, which were protected by an insulating paint, were prepared by galvanostatic electrolysis in the supporting electrolyte. A Rigaku-Rotaflex diffractometer using monochrome CuK_α radiation at 50 kV and 140 mA was employed to obtain strip chart recording from 2θ = 5 to 80° at 2° min^{-1}.

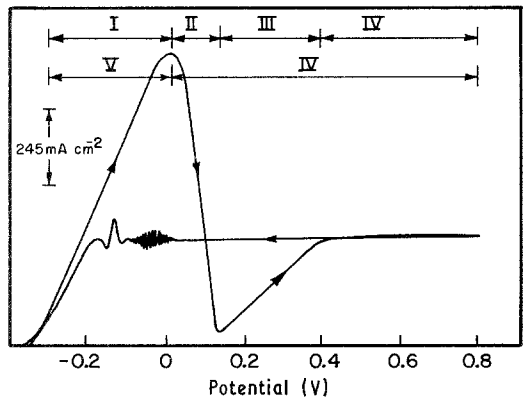

Fig. 2. Cyclic voltammogram of Cu–As (0.15% (w/w)) electrode in 1.66 M H_2SO_4, 0.29 M $NiSO_4$ and 0.66 M $CuSO_4$. $v = 20\,mV\,s^{-1}$, $T = 65.0 \pm 0.5°C$. The potential sweep was started at $E_{i=0} = -340\,mV$ vs Hg, Hg_2SO_4/K_2SO_4 standard reference electrode. (I) Active dissolution; (II) prepassivation; (III) prepassive dissolution; (IV) passivation; (V) rupture of passivity and reactivation.

The SEM analyses were performed using a JEOL JSM-25S microscope, equipped with a TN 5700 model energy dispersive X-ray (EDX) analyzer (Tracor Northern Co.). The samples were prepared galvanostatically and washed thoroughly with distilled water. They were coated by a thin layer of gold–palladium before the SEM measurements.

3. Results and discussion

3.1. *Electrochemical studies*

3.1.1. Cyclic voltammetry studies. Figure 2 shows the current–voltage plot derived from cyclic voltammetric measurements for the dissolution of a copper–arsenic electrode in 1.66 M sulphuric acid solution. As the applied potential is swept anodically, the current rises exponentially (when *IR* corrections are made) until a maximum is reached (region I). This is attributed to the active dissolution of copper.

The general polarization characteristics show a peak current followed by a current minimum at potentials above the apparent Tafel region, corresponding to a prepassivation step (region II). As the potential is driven to more positive values, the current rises linearly to reach a nearly constant level (prepassive dissolution (region III)) and this plateau extends to ca 0.8 V vs MSE. This constant current regime corresponds to the passivation of the electrode (region IV). The current remains nearly constant during the cathodic retrace for a larger potential range (0.8–0.0 V vs MSE). Below 0.0 V vs MSE, sustained current oscillations are observed followed by a periodic double oscillation indicating a reactivation of the electrode (region V).

While the chaotic oscillations were observed for all electrodes, the periodic sine wave-shaped single oscillation is very characteristic of the Cu–As electrodes and has never been observed for any arsenic-free electrodes.

3.1.2. Impurities and effect of dissolved gases. The present trend for understanding passivation phenomena is to accept the formation of a film at the electrode surface as being responsible for the passivation [14]. The film growth should be sensitive to the nature of the dissolved gases in the solution and the impurities present at the electrode interface. The anodic behaviour of Cu, Cu–As and Cu–Sb was found to be affected by the nature of dissolved gases, as can be seen from Fig. 3. The time delay to passivation is estimated by cycling the electrode potential, which is equivalent to a long-time electrolysis (Fig. 4). Comparison of the peak current density values, i_p, for the first and tenth cycles gives an estimation of the tendency of the electrode to passivation. The different data obtained from Fig. 3 are summarized in Table 1.

Oxygen appears to delay the passivation process, as evidenced in the cyclic voltammetric studies. The more oxygen present in solution, the better the anodic dissolution of copper. The diminution of peak current was the lowest in oxygen-saturated solutions. This is in very good agreement with Leckie's results [15]. On the other hand, antimony-containing electrodes were found to passivate more easily than those containing arsenic. The susceptibility to passivation decreases in the following order: Cu–Sb > pure Cu > Cu–As, in the following media: N_2 saturated > air saturated > O_2 saturated.

Table 1. Comparison between the different peak current densities and limiting current densities, respectively, for the three electrodes in different atmospheres, data obtained from Fig. 3

	Pure copper			*Copper–antimony*			*Copper–arsenic*		
	A	*B*	*C*	*A*	*B*	*C*	*A*	*B*	*C*
$i_p(1)$ (mA)	611	675	618	587	607	538	611	587	551
$i_p(10)$ (mA)	490	532	518	504	549	497	554	587	647
$\Delta i_p/i_p(1)$ %	23.5	21	16	31	10	8	9	0	−22
$i_{lim}(1)$ (mA)	261	303	238	228	232	212	292	281	244
$i_{lim}(10)$ (mA)	217	242	223	204	204	218	212	265	265
$\Delta i_{lim}/i_{lim}(1)$ (%)	17	20	6	11	12	−3	27	6	−9
$[(\Delta i)/i]_{av.}$	18.5	20.5	11	21	11	2.5	18	3	−15

$\Delta i_p = i_p(1) - i_p(10)$, $\Delta i_{lim} = i_{lim}(1) - i_{lim}(10)$ and $[(\Delta i)/i]_{av} = [(\Delta i_p/i_p) + (\Delta i_{lim}/i_{lim})]/2$.
(A) Solution saturated with nitrogen; (B) solution as first introduced; (C) solution saturated with oxygen.

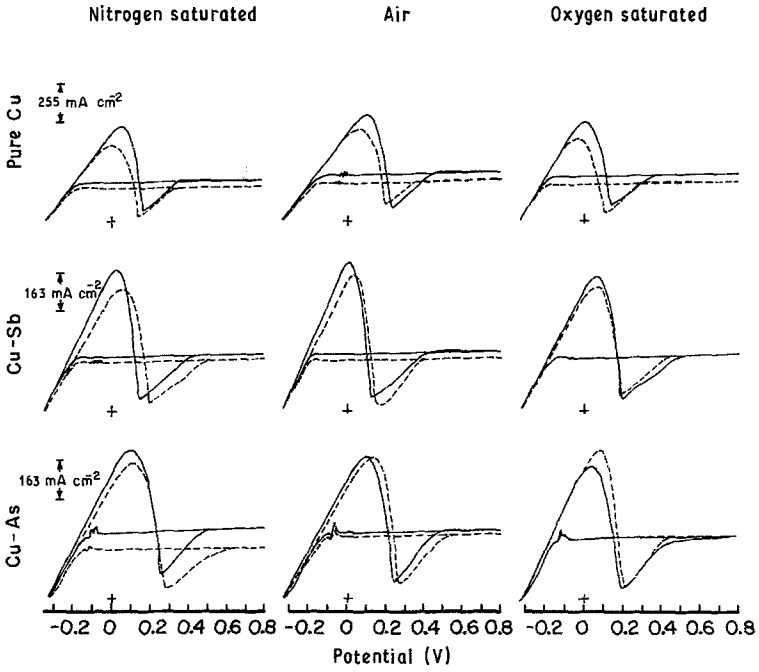

Fig. 3. Cyclic voltammograms of (A) pure copper, (B) Cu-(0.055% (w/w)) Sb, (C) Cu-(0.15% (w/w)) As electrodes in electrolytes with different oxygen content. The experimental conditions are the same as in Fig. 2.

Many hypotheses for the mechanism of the anodic behaviour of copper in acidic media have already been reported. Accumulation of insulating or semiconducting oxide layers on the electrode active surface may be one parameter responsible for the passivation. Oxygen acts as an oxidizing agent for Cu^+ cations and can dissolve the cuprous oxide (Cu_2O) layer by forming a cupric oxide (CuO) which in turn dissolves in the highly acid medium according to the following reaction scheme:

$$Cu_2O + 1/2O_2 \longrightarrow 2CuO$$

$$CuO + 2H^+ \longrightarrow Cu^{2+} + H_2O$$

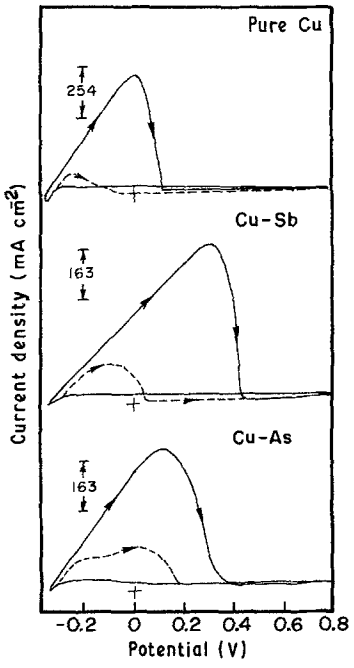

Fig. 4. Cyclic voltammograms of (A) pure Cu, (B) Cu-Sb, (C) Cu-As electrodes after passivation was reached by imposing a constant current (i = 40 mA cm^{-2}). The working electrode was set in an upward-faced horizontal position.

which can be rewritten, taking into account the sulfate anions as:

$$Cu_2O + 2H_2SO_4 + 1/2O_2 \longrightarrow 2CuSO_4 + H_2O$$

$$\Delta G^0 = -47.3\,\text{kcal mol}^{-1}$$

3.1.3. Oscillations and gravity. The oscillations which can occur at the onset of the anodic current regime are one of the more intriguing features of the copper sulphuric acid system. A model often invoked to explain this behaviour postulates the formation and dissolution of a partially soluble, inhibiting surface layer [16, 17]. While the formation of such a layer may be a necessary condition, it is not sufficient in itself to explain the oscillatory behaviour. We found it desirable to re-examine the voltammetric characteristics of this system, since the overall mechanism remains poorly understood.

The oscillatory anodic behaviour of copper in chloride media under hydrodynamic conditions has been examined with rotating disc electrodes [14]. This technique does not allow the separation of the different forces responsible for the film removal from the surface. That is, the nature of the forces cannot be distinguished, and only the resultant of the centrifugal force due to the hydrodynamic, thermal convections and the gravity forces can be estimated. Central to this issue is the study of the dependence of the oscillatory phenomenon on the position of the stationary working electrode. Besides the conventional position where both the counter and working electrodes were set in a vertical position, the working electrode was set in an upward-facing horizontal position at the bottom of the cell. This configuration allowed an evaluation of the contribution of the gravitational force to the oscillatory phenomenon.

The cyclic voltammograms obtained for the three electrodes in both positions are presented in Fig. 5. The amplitude of the oscillations decreased markedly

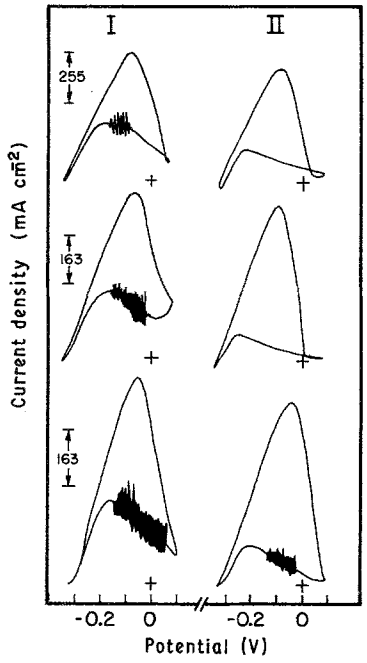

Fig. 5. Cyclic voltammograms of (A) pure copper, (B) Cu–(0.055% (w/w)) Sb, (C) Cu–(0.15% (w/w)) As electrodes. (I) The electrode was set in a vertical position; (II) the electrode was set in an upward horizontal position. The experimental conditions are the same as for Fig. 2.

when the electrode was set in the horizontal position. The peak current densities were smaller when the electrode was set in the horizontal position. This might be explained in terms of electrode active area. In fact, powderous slime layers were always observed on Cu, Cu–Sb electrodes, and a more rigid, black film on the surface of Cu–As electrodes. For the vertical working electrode position, the deposit fell off the electrode surface to form the so-called slime on the bottom of the cell. The removal of the non-conducting film from the electrode leaves micro-surfaces which leads to very high current densities. A high localized gradient of concentration is thus produced and leads to a rapid formation of non-conducting slime layer. The repetition of this phenomena is observed on the cyclic voltammograms as current oscillations.

Moreover, the magnitude and the nature of the oscillations were found to be very dependent on the high limit value of the scanning potential. That is, during the reverse voltammetric sweep, the oscillations may or may not be observed depending on the limit where the potential has been reversed. A critical potential of 100 mV vs MSE for which the oscillations were extremely strong, was observed (Fig. 6).

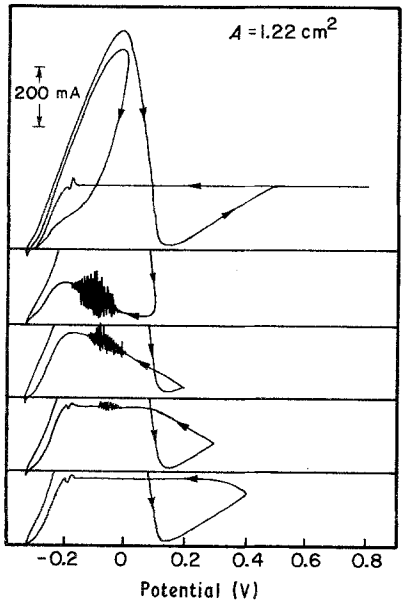

Fig. 6. Magnitude of current oscillation for different high limit scanning potentials.

3.1.4. Kinetic of the anodic behaviour of copper. Cyclic voltammetry provides some very useful information; for instance, the study of the dependence of peak current density (i_p) on the potential sweep rate aids in understanding the laws which govern the electrode kinetic mechanism. The anodic behaviour of copper is diffusion controlled since the peak current densities vary linearly with respect to the square root of potential sweep rates in two separate domains (Fig. 7). As the mechanism remains not well understood, it is impossible to evaluate the diffusion coefficient with any accuracy. The peak current density for semi-infinite linear diffusion is given by the following relationship [18]:

$$i_{peak} = 0.4463nFC_i^* \left(\frac{nF}{RT}\right)^{1/2} D_i^{1/2} v^{1/2} \qquad (1)$$

Applying this relationship to the obtained results for the arsenic-containing samples leads to values of $(n^{3/2}C_iD_i^{1/2})^2 = 8.39 \times 10^{-11}$ and 2.82×10^{-11} from each slope. Considering a bi-electronic reaction ($n = 2$) and taking $C_i = C_{Cu^{2+}} = 0.66 \times 10^{-3}$ mol cm^{-3}, the average values of $D_{Cu^{2+}} = 2.41 \times 10^{-5}$ and 0.81×10^{-5} cm^2 s^{-1} were obtained. Moreover, the unusual break in the slope of i_p vs $v^{1/2}$ was attributed to a change of the medium viscosity following the high concentration gradient imposed by the fast sweep rates ($v > 50$ mV s^{-1}).

3.2. *X-ray and SEM analysis*

X-ray diffraction analysis (XRDA) spectroscopy can provide qualitative information on the chemical

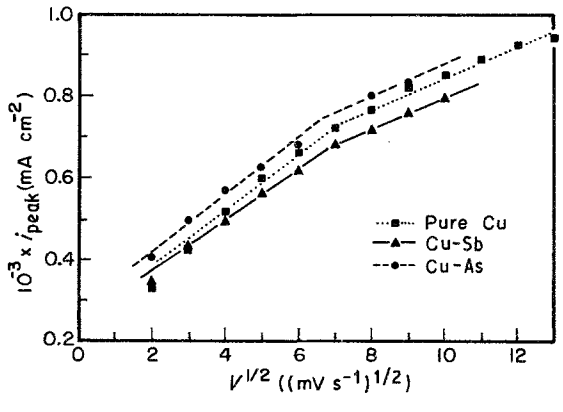

Fig. 7. Peak current density evolution with respect to the square root of the potential sweep rate for (A) pure Cu, (B) Cu–Sb, (C) Cu–As fresh electrodes.

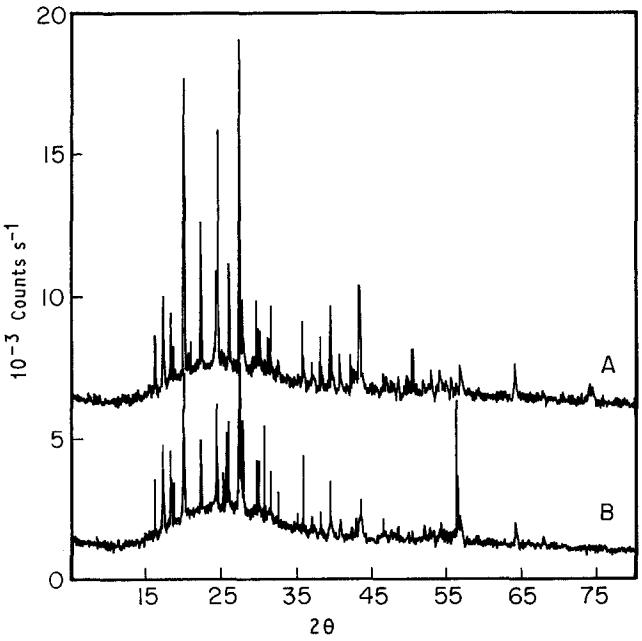

Fig. 8. X-ray spectra for (A) Cu–Sb and (B) Cu–As samples. The specimen were polarized galvanostatically in the base solution.

species present at the surface of an electrode and furnishes a rapid and accurate method for identification of crystalline phase present in a material [19, 20]. Typical XRDA results are shown in Fig. 8.

The chemical species detected were copper metal at all electrodes and copper sulphate pentahydrate for arsenic-containing electrodes and copper sulphate trihydrate for antimony-containing electrodes. Many other phases which were expected to be present (e.g. cuprite) were surprisingly not detected. The corresponding lines were not existent or were significantly weak. The lack of observation of other species, despite the presence of very dark substances on the electrode surfaces, may be due to a low concentration of species or to their crystallographic properties. Amorphous phases are transparent to the X-ray diffraction technique. This result was not surprising since only copper showed strong crystallographic peaks during XRDA tests conducted on blank non-electrolyzed samples. The latter suggested that the impurities were completely dissolved within the copper matrix.

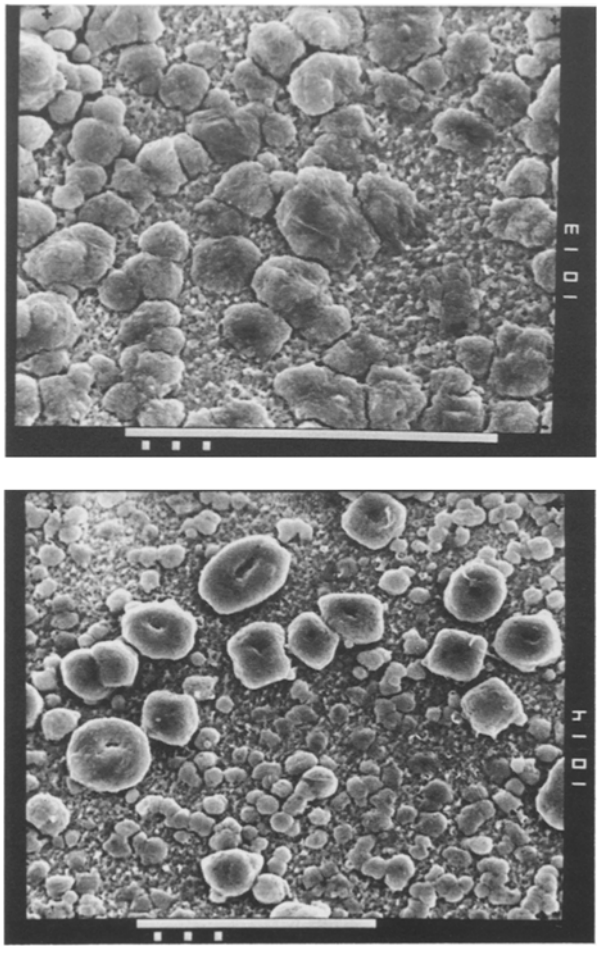

Fig. 9. SEM micrographs obtained on galvanostatically polarized electrodes at 100 mA for 24 h. (a) Antimony-containing samples; (b) arsenic-containing samples.

In an attempt to perform a better X-ray identification of the elements present, scanning electronic microscopy (SEM) and energy dispersive X-ray (EDX) analysis were carried out. Figure 9 shows the SEM micrographs obtained on the respective electrodes after a galvanostatic polarization at 100 mA for 24 h. It shows dominant white snowball-shaped features on a darker background. EDX measurements performed on both the bright and darker regions are shown in Fig. 10. Sulphur, as well as nickel from the solution, were revealed with copper, as can be seen from the spectral peaks at 2.35 keV for S, 7.47 keV for Ni and 0.92, 8.03, 8.89 for Cu (Fig. 10a, I, II). The remaining darker region was composed mainly of copper-containing compounds or metallic copper (Fig. 10b, I, II).

Unfortunately, the EDX measurements do not allow the identification of the oxidation state of the elements. Copper sulphate has been previously reported to be responsible for the passivation of copper anodes. The actual XRDA results revealed $CuSO_4 \cdot xH_2O$ in both arsenic- and antimony-containing electrodes. It is noted that the nickel was not observed in the regions where sulphur was not detected (Fig. 10).

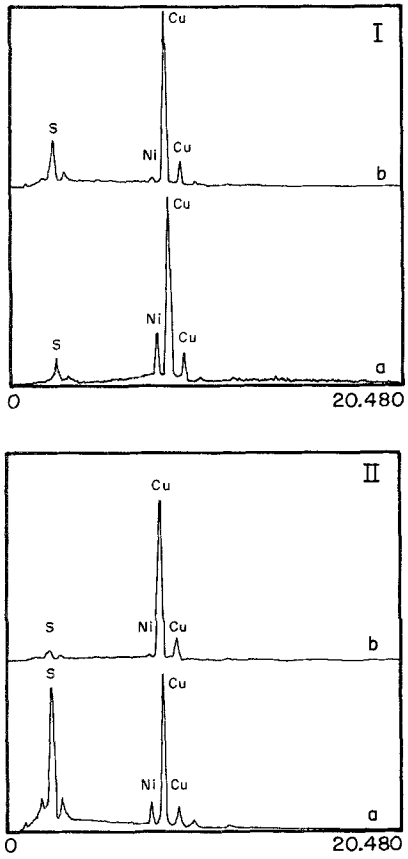

Fig. 10. EDX analysis spectra obtained on: (I) Cu–Sb, (II) Cu–As. (a) The spectrum is obtained from the bright region (see Fig. 9a); (b) the spectrum is obtained from the dark region (see Fig. 9b).

4. Conclusions

The presence of impurities such as arsenic in the electrode as well as oxygen in the solution has been strongly demonstrated to be beneficial to the electrorefining process.

The kinetics of the anodic process of these electrodes (pure Cu, Cu–As, Cu–Sb) has been demonstrated, using cyclic voltammetry, to be diffusion controlled. The diffusion constant of Cu^{2+} in the industrial supporting electrolyte was found to be affected by the potential scan rate. An average value of $D_{Cu^{2+}} = 2.38 \times 10^{-5} cm^2 s^{-1}$ was found for low scan rates ($v < 50 mV s^{-1}$) while for higher scan rates ($v > 50 mV s^{-1}$) the value did not exceed $0.77 \times 10^{-5} cm^2 s^{-1}$. Higher scanning rates cause high variation of concentrations which leads in turn to an increase of the medium viscosity.

The present investigation also clearly demonstrates the role of gravity in the oscillatory behaviour of copper anodization. The oscillations are caused by the formation and precipitation of non-conducting films from the surface under the influence of their weight only.

Some surface analysis results showed the presence of copper sulphate crystals, metallic copper and copper oxides (cuprite) on the surface of electrolyzed electrodes.

Acknowledgements

The authors wish to express their thanks to Dr P. L. Claessens and Mr V. Baltazar (Noranda Research Center, Montreal) for their contribution and interest. The financial support of the National Sciences and Engineering Research Council of Canada (NSERC) and the Noranda Mines Limited is gratefully acknowledged.

References

[1] G. Milazzo, 'Electrochimie', Edt. Dunod, Paris (1969) p. 13 (Tome 2).
[2] S. Abe, B. W. Burrow and V. A. Ettel, *Can. Metal. Quart.* **19** (1980) 289.
[3] L. Kiss, M. L. Varsanyi and A. Bosquez, *Hung. Chem. J.* **87** (1981) 504.
[4] A. A. Yun, I. B. Murashova and A. V. Pomosov, *Sov. Electrochem.* **9** (1973) 443.
[5] D. Schab and K. Hein, *Neue Hutte* **19** (1970) 408.
[6] S. Abe, S. Goto, *J. Mining Metal. Inst. Jap.* **97** (1981) 479.
[7] T. T. Chen and J. E. Dutrizac, 'The Electrorefining and Winning of Copper' TMS-AIME, Warrendale, PA (1987) p. 499.
[8] J. C. Minotas, H. Djellab and E. Ghali, unpublished results.
[9] Y. Umetsu and S. Suzuki, *J. Mining Metal. Inst. Jap.* **77** (1961) 882.
[10] J. Sedzimir, *Non-Ferrous Ores Metals* **25** (1980) 415.
[11] S. Abe and S. Goto, *J. Mining Metal. Inst. Jap.* **97** (1981) 549.
[12] V. Baltazar, P. L. Claessens and J. Thiriar, '*The Electrorefining and Winning of Copper*', TMS-AIME, Warrendale, PA (1987) p. 211.
[13] O. Forsen and M. H. Tikkanen, *Scand. J. Metal.* **10** (1981) 109.
[14] H. P. Lee, K. Nobe and A. J. Pearlstein, *J. Electrochem. Soc.* **132** (1985) 1031.
[15] H. P. Leckie, *J. Electrochem. Soc.* **117** (1970) 1478.
[16] H. H. Uhlig, *Corros. Sci.* **19** (1979) 777.
[17] T. P. Hoar, *Corros. Sci.* **7** (1967) 341.
[18] A. J. Bard and L. R. Faulkner, 'Electrochemical Methods', Wiley, New York (1980) p. 218.
[19] J. H. Schloen, *C.I.M. Bull.* **79** (1986) 102.
[20] H. D. Speckman, S. Haupt and H. H. Streblow, *Surface Interf. Anal.* **11** (1988) 148.